

INVESTIGATING ASME ALLOWABLE LOADS WITH
FINITE ELEMENT ANALYSES

Miguel Mattar Neto; Luciano M. Bezerra;
Carlos A. de J. Miranda; Julio R. B. Cruz;

Comissão Nacional de Energia Nuclear/SP-IPEN
Travessa R, 400. Cidade Universitária, USP, 05508-900
São Paulo - SP. Tel.: (011) 816-9437. Fax (011) 212-3546



COLEÇÃO PTC
DEVOLVER AO BALCÃO DE EMPRÉSTIMO

ABSTRACT

The evaluation of nuclear components using finite element analysis (FEA) does not generally fall into the shell type verification adopted by the ASME Code. Consequently, the demonstration that the modes of failure are avoided sometimes is not straightforward. Allowable limits, developed by limit load theory, require the computation of shell membrane and bending stresses. How to calculate these stresses from FEA is not necessarily self-evident. One approach to be considered is to develop recommendations in a case-by-case basis for the most common pressure vessel geometries and loads based on comparisons between the results of elastic and plastic FEA. In this paper, FE analyses of common 2D and complex 3D geometries are examined and discussed. It will be clear that in the cases studied, stress separation and categorization are not self-evident and simple tasks to undertake. Certain unclear recommendations of ASME Code can lead the stress analyst to non conservative designs, as will be demonstrated in this paper. At the end of this paper, taking into account comparison between elastic and elastic-plastic FE results from ANSYS some observations, suggestions and conclusions about the degree of conservatism of the ASME recommendations will be addressed.

RESUMO

Em geral, para a avaliação de componentes nucleares, usando resultados obtidos a partir de modelos de elementos finitos sólidos 2D e 3D, não é possível a aplicação direta do Código ASME. Valores admissíveis, obtidos com base em análise limite, requerem o cálculo de tensões de casca de membrana e de flexão. Recomendações para a avaliação de tensões em análises 2D e 3D podem ser obtidas pela comparação entre resultados de análises elásticas e plásticas usando-se elementos finitos. Neste trabalho são apresentados casos 2D e 3D analisados elástica e plasticamente com o ANSYS. A separação e a classificação de tensões, de acordo com o Código ASME, são discutidas e algumas recomendações são, também, apresentadas.

7º Seminário de Elementos Finitos, São Paulo, SP, 27-29 de setembro de 1995.

INTRODUCTION

The main standard for the design of nuclear pressure vessels and piping is the ASME code [7]. In the whole world, such a code is simply adopted, fitted, or copied as the major requirement for pressure vessel design. In the early 60's, the ASME, with considerable foresight, recognized the advantages of detailed stress analysis. Thereupon, the ASME introduced the so-called "design by analysis" route which was deliberately set up for nuclear applications [8]. The rules formulated in the "design by analysis" approach were based upon concepts from plasticity in an attempt to avoid mainly the consequences of possible bursting or ratcheting failure and fatigue. This approach required an elastic analysis of the vessel or component (although it did not restrict design to elastic analysis alone) and the separation and classification of the calculated shell type stresses. The stresses were categorized into primary, secondary, and peak stresses and different design allowables were applied according to the failure mode to be avoided.

The method of stress calculation was not specified, although it was clear at the time that shell discontinuity analysis was seen as the main method of analysis. The dominant problem in "design by analysis" is that of categorization of stresses. The rules governing stress categorization are not precise, but experience and common practice coupled with the use of thin shell calculations have allowed some degree of reliability to be introduced into the design process.

However, if the elastic analysis is performed using more detailed continuum finite element calculations, which is a very common practice today, then the categorization of the stresses and the extraction of shell type through wall membrane and bending stresses, primary and primary plus secondary, becomes difficult.

Both primary and primary plus secondary stress limits involve transition from elasticity to plasticity. Using limit load theory, elastic limits are readily defined for simple structures under simple loading (e.g. beams under tension or bending loads). Also, shells of revolution can be reasonably evaluated for elastic limits. Once the elastic limits are known, guidelines can be written for performing elastic analysis that assures conservatism while giving reasonably accurate solutions relative to the limit load solution. Once the guidelines are established, the designer can clearly demonstrate that the limits on the modes of failure have been met.

MOTIVATION

The evaluation of components using finite element analysis (FEA) does not generally fall into the shell type verification cookbook. Consequently, the demonstration that the modes of failure are avoided sometimes is not straightforward. Elastic rules, developed by limit load theory, require the computation of the shell type through wall membrane and bending stresses. How to calculate these stresses from 2D and 3D FEA is not necessarily self-evident. The general opinion of pressure vessel designers is that current techniques can provide safety comparable to current axisymmetric evaluations. This common approaches appear to be based more on a hoped-for conservatism rather than accuracy.

The expectation that the widespread use of FEA would displace more simplified methods of analysis in pressure vessel and piping design was not confirmed. On the contrary, the need for simplified methods had become even greater. The main reason for this trend is that FEA (axisymmetric and 3D) generates results that often need expertise to reinterpret them in order to make engineering assessments and stress evaluations. The main question to be answered is how to assess the structural design of pressure vessels from an elastic FEA considering that the failure modes to be avoided are closely related to plastic (nonlinear) effects. One approach to be considered is to develop recommendations in a case-by-case basis for the most common pressure vessels geometries and loads based on comparisons between the results of elastic and also plastic FEA. This proposal is indicated in Hollinger and Hechmer [9] considering that ASME code assessment of stress limits for complex geometries and loading conditions requires a clear understanding of the relationship between stress categories and failure mechanism relation to them, the appropriate stresses for each stress category, the appropriate locations for assessing stresses, and the approach used to calculate membrane plus bending stresses (to linearize stresses) in FEA.

In this paper, following the indication given in [9], three axisymmetric skirt supports and lugs attached to a cylindrical pressure vessel wall are examined and discussed in detail. The skirt configurations here analyzed are typical structures where the influence of stress assessment and classification can be clearly observed. The case of the lug geometry is a typically case of a 3D configuration where coping with the requirements of the ASME is not a simple task. From the comparison of the FEA results in elastic and elastic-plastic regimes, using the ANSYS program [10], some conclusions about ASME allowable limits can be undertaken.

AXISYMMETRIC ANALYSES

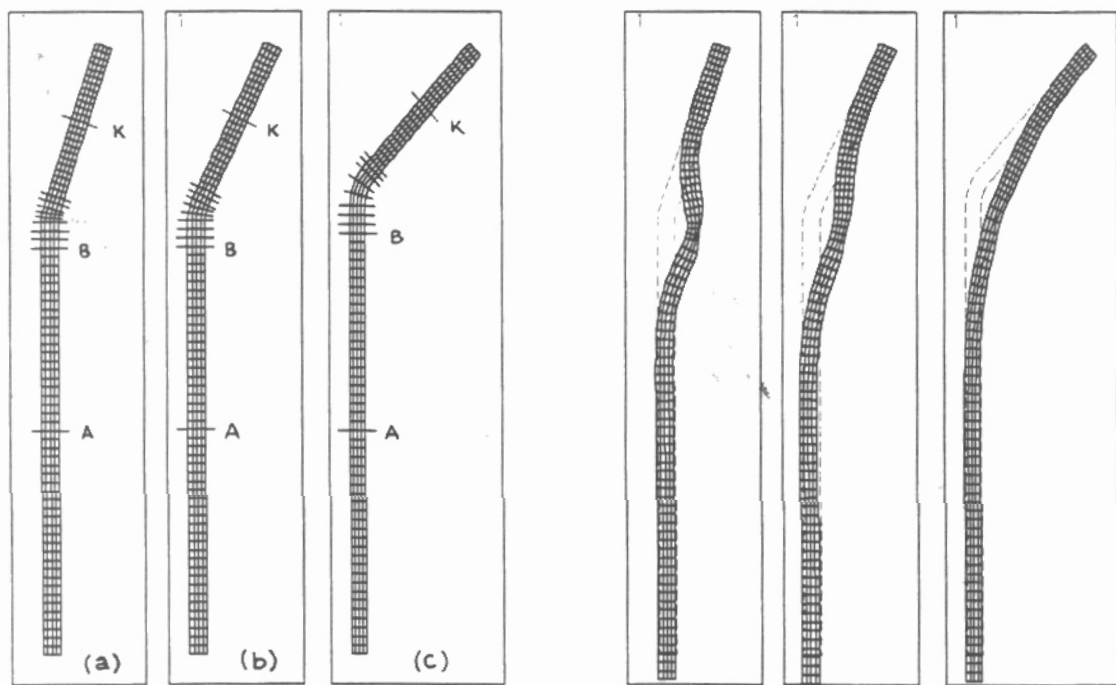
Three support skirts assembled with cylinders and cones linked with different attachment angle α (with respect to the central axis) are analyzed. Different skirts with different α angles are used so that the impact of diverse bending values on the limit loads can be investigated. At the end of the cylindrical part, an arbitrary axisymmetric stress of $F = 1122\text{psi}$ acting on the inferior cross section of the cylinder is applied. The FE meshes of the skirts are depicted in Figure 1.

The cone upper part is completely fixed to simulate a rigid foundation. Also the nodes at the inferior section of the cylindrical part - where the end-load is applied - are coupled to simulate zero rotation. Taking into account the geometric change cone-cylinder and the locally applied stress at the bottom of the cylinder, an attenuation length of $s\sqrt{Rt}$ is considered. A blend radius of $2t$ in the juncture notch cylinder-cone is also used. Thus stress singularity in the notch can be prevented.

The arbitrary end-load stress of 1122psi in the support skirts, causes only elastic stresses in the skirts. Figure 1 also shows the stress classification lines "SCL," where the elastic stresses are linearized. Other than verifications with elastic analysis, the ASME Code also admits the use of the plastic analysis. The limit analysis is a special case of plastic analysis taking the material as ideally plastic with no strain hardening. Considering a structure made of such material, a

lower bound collapse load can be defined as the maximum load that such a structure can carry without an unbound increase of deformations. For the knowledge of the limit load of each skirt configuration, the lower bound collapse approach is used. It was assumed a stress-strain curve with an initial slope of $E = 29.5 \times 10^6 \text{psi}$, and a stress plateau at $S_y = 40,000 \text{psi}$. Accepting two-thirds of the lower bound collapse load is compatible with the ASME Code requirements to find the allowable load based on limit analysis. The classical bilinear option from ANSYS with the Von Mises yield surface flow law was employed in the inelastic FE model. Very small load steps are adopted during the plastic analysis of the structures. For the skirts, an end-load increment of 100psi is applied. The ANSYS default convergence criterion is adopted during the typical 10 iterations used for each load step increment.

Using ANSYS, the limit-loads of each skirt configuration is determined and compared with the diversity of loads allowed by the ASME Code when different stress classification approach is used. It will be possible to observe the influence of the support skirt attachment angle between cone-cylinder on the allowable loads. The influence of the bending stress classification on the failure mode can also be observed. The degree of conservatism of the ASME Code can be checked. Also in Figure 1, the deformation of each skirt on the onset of the collapse is shown. Table-A summarizes the collapse loads for each skirt configuration.



material with $E = 29.5 \times 10^6 \text{psi}$, $\nu = 0.3$, $S_m = 26,700 \text{psi}$, $S_y = 40,000 \text{psi}$
 internal radius $R_i = 48.64 \text{in}$; thickness $t = 2 \text{in}$

Figure-1 - (a) Skirt with $\alpha=18^\circ$, (b) Skirt with $\alpha=25^\circ$, (c) Skirt with $\alpha=45$ and the respective deformations on the onset of the collapse.

From Table-A, it is straightforward that the bigger the attachment angles α are, the smaller the collapse loads are. Thus, it should be reasonable to treat at least some share of the membrane + bending stress as primary stress [1] but the code considers, in areas of geometric discontinuity, membrane as local and bending as secondary.

TABLE-A- Summary of the collapse loads

Component Analyzed	Collapse Load
Skirt angle $\alpha=18^\circ$	36300 psi - end load
Skirt angle $\alpha=25^\circ$	30700 psi - end load
Skirt angle $\alpha=45^\circ$	18700 psi - end load

ASME ALLOWABLES - AXISYMMETRIC CASES

The philosophy of "adequate safety" that is granted by the limits imposed to general primary membrane ($S_y + 1.5$ or S_m) and primary membrane-plus-bending stress (S_y or $1.5 S_m$) in the ASME Code is based on the simple beam theory. Following the steps presented in [1], the "simple" collapse loads of the skirts analyzed are set when the axial membrane stress, hypothetically, reaches the yielding stress value $S_y = 40,000\text{psi}$. Considering the safety factor of 1.5, the allowable end-loads for all the skirt configurations are then obtained after dividing S_y per 1.5; that is: $26,700\text{psi}$.

Using ANSYS FE package a more precise value for the collapse loads can be achieved as can be seen in Table-A. For the skirt with $\alpha=18^\circ$, the FEA results confirm the values given in [1]. From the elastic FEA it can be observed that in the vicinity of the cylinder-cone juncture, the maximum membrane stress intensity is in SCL-J. The stress intensity in SCL-J is dominated by meridional stress and reaches the value of 1153psi . In the bending region cylinder-cone, the membrane stress can be classified as a local stress (P_L). The Code rule limits local stress $P_L \leq 1.5S_m=40,000\text{psi}$. Thus, if the end-load of 1122 causes $P_L=1153\text{psi}$, the maximum allowable end-load is then $40000 \times 1122 \div 1153 = 38924\text{psi}$. Analogously for the skirt with $\alpha=25^\circ$, the maximum P_L stress intensity is at SCL-E and $P_L=1562\text{psi}$. In this case the maximum allowable end-load is $40000 \times 1122 \div 1562 = 28732\text{psi}$. Similarly, for the skirt with $\alpha=45^\circ$ the maximum P_L is SCL-E and $P_L=3066\text{psi}$. In such a case, the maximum allowable end-load, based on ASME local membrane limit, is $40000 \times 1122 \div 3066 = 14637\text{psi}$.

From the elastic FEA of ANSYS, the maximum values of ($P_L + P_B$) are: 2839psi in SCL-F for the skirt with $\alpha=18^\circ$, 3457psi in SCL-F for $\alpha=25^\circ$, and 5349psi in SCL-G for $\alpha=45^\circ$. Considering membrane+bending as primary stresses, the Code limits $P_L + P_B \leq 1.5S_m=40000\text{psi}$. Taking such limiting value, the allowable end-loads for the skirts are: a) $40000 \times 1122 \div 2839 = 15808\text{psi}$ for the skirt with $\alpha=18^\circ$, b) $40000 \times 1122 \div 3457 = 12982\text{psi}$ for the skirt with $\alpha=25^\circ$, and c) $40000 \times 1122 \div 5349 = 8390\text{psi}$ for the skirt with $\alpha=45^\circ$.

The ASME Code considers the bending stress in the cylinder-cone transition as secondary. Categorizing the membrane+ bending as primary+secondary stress, the Code limits $P_L+P_B \leq 3S_m = 80000 \text{ psi}$. Therefore, in such a case the allowable end-loads are the double of the values obtained before, i.e., 31616 psi , 25964 psi , and 16780 psi , for the skirts with $\alpha = 18^\circ$, 25° , and 45° , respectively. It should be noted that if $P_L+P_B > 3S_m = 80000 \text{ psi}$ appropriate penalty factors should be applied for the fatigue evaluation, and ratcheting should be prevented. The results are summarized in Table-B.

TABLE - B - Summary of the stresses from elastic analyses

		End-Loads (psi)								
		Cone with 18			Cone with 25			Cone with 45		
		At Limit	Allowable	SCL	At Limit	Allowable	SCL	At Limit	Allowable	SCL
Beam Theory		40000	26700	----	40000	26700	----	40000	26700	----
FEA	M as PM	38425	25616	A	37809	25206	A	36019	24013	A
	M as PL	38924	38924	J	28732	28732	E	14637	14637	E
	M+B as PL+PB	15808	15808	F	12982	12982	F	8390	8390	G
FEA	M as PM	38425	25616	A	37809	25206	A	36019	24013	A
	M as PL	38924	38924	J	28732	28732	E	14637	14637	E
	M+B as P+Q	31616	-----	F	25964	-----	F	16780	-----	G
FEA, Limit Load		36300	24200	----	30700	20466	----	18700	12467	----

TRIDIMENSIONAL ANALYSES

The tridimensional analyses of this paper concern a cylindrical pressure vessel with two symmetric radial lugs under different loading conditions. ANSYS FE models, taking advantage of the symmetries of geometry and loading, are used for the elastic and also elastic-plastic analyses. The applied loads considered in the analyses are: internal pressure in the cylindrical shell, radial and axial forces acting on the lugs. The forces directions refer to the cylindrical shell coordinate system. The geometric and material characteristics of the region of the lug-cylinder attachment are presented in Figure 2 together with one of the finite element model used during the stress analyses.

Two finite element models were built for the stress analyses. The first model can be seen in Figure 2 and was used for the stress evaluation of the structure under internal pressure plus the axial force on each lug. In this case, taking credit of the cylinder-lugs attachment symmetry and the symmetry of the axial force, only a quarter of the structure was discretized.

ASME ALLOWABLES - TRIDIMENSIONAL CASES

From the elastic-plastic FEA results, the forces on the lugs that cause the collapse of the lug-cylinder attachment can be summarized in Table C.

TABLE C: Collapse forces in the lugs (MN), from elastic-plastic FEA

Radial forces in the lugs	with internal pressure	2.72
	without internal pressure	2.65
Axial forces in the lugs	with internal pressure	1.58
	without internal pressure	1.53

To find the allowable load value, the recommendations of "NB-3228 Applications of Plastic Analysis" of the ASME code was followed. Therefore, applying the factor 2/3 to the collapse loading combination, the allowable loads are summarized in Table D.

TABLE-D: Allowable load conditions, from elastic-plastic FEA

Radial forces in the lugs	with internal pressure	$p = 10 \text{ MPa} +$ $F = 1.82 \text{ MN}$
	without internal pressure	$F = 1.77 \text{ MN}$
Axial forces in the lugs	with internal pressure	$p = 10 \text{ MPa} +$ $F = 1.05 \text{ MN}$
	without internal pressure	$F = 1.02 \text{ MN}$

If the designer uses a simple elastic FE analysis to evaluate the shear in the lugs and in the shell, the recommendations of "NB-3227.2. Pure Shear" of the ASME code have to be followed. In this situation, the allowable forces in the lugs are 4.42 MN and 1.11 MN for the radial and the axial directions, respectively. Notice that those allowable forces were found considering the average shearing stresses on the strength sections of the structure. The shearing stresses correspond to the situation of the lug punching the shell for the lug under radial force and the lug tearing out from the shell for the lug under axial force. Comparing those results to the values from Table D one may conclude that the simplified elastic analysis shows good agreement in the case more close to pure shear which corresponds to the axial force on the lug. In the situation of shell punching (radial forces on the lug) the results do not agree. In this case it can be concluded that the elastic analysis may lead to non-conservative design.

To compare the results from elastic and elastic-plastic FEA it is necessary to define the loads from elastic FEA corresponding to the allowable stress limits prescribed by the ASME code. Therefore, in the case of elastic FEA, it is always necessary to separate and classify the finite element stresses in shell type stresses. In other words, the FE stresses have to be divided and categorized into wall membrane and bending stresses. However, as mentioned in the Introduction

of this paper, there is no established procedure to perform this categorization in 3D finite element models. In this work, it was followed the recommendations of Hechmer and Hollinger [6] and the so-called "linearization by a line". The lines (L) were chosen at the shell body and at distances away from the edge of the lug attachment. The distances were taken as $0.1\sqrt{Rt}$, $0.5\sqrt{Rt}$, $1.0\sqrt{Rt}$, and $2.0\sqrt{Rt}$, respectively for the lines L1, L2, L3, and L4. R is the mean radius of shell, and t its thickness. Applying the load conditions shown in Table D, from the elastic analyses, the membrane stress intensities shown in Table E can be obtained. .

TABLE-E: Membrane stress intensities (MPa), from elastic FEA

		L1 - $0.1\sqrt{Rt}$	L2 - $0.5\sqrt{Rt}$	L3 - $1.0\sqrt{Rt}$	L4 - $2.0\sqrt{Rt}$
radial forces in the lugs	with pressure (10MPa)	347	141	115	149
	without pressure	377	202	124	54
axial forces in the lugs	with pressure (10 MPa)	105	107	108	131
	without pressure	16	18	24	54

According to NB-3213.10 "Local Primary Membrane Stress" of the ASME code, one can see from the results of Table E that, for the loading conditions used, the stressed region may be considered local because the membrane stress intensities that exceed $1.1 S_m = 202$ MPa do not extend more than $1.0\sqrt{Rt}$. The forces in the lugs may even be increased and the condition to consider the region as a place of local membrane stress remains satisfied. For example, in the case of radial force only, the value may be increased from 2.65 MN to 2.89 MN = $(1.77/124) \times 1.1 S_m$.

In the cases of axial forces in the lugs, the stresses in the shell are little influenced by the gross geometric discontinuity between lug and shell. As we are more concerned with the shell evaluation and the stresses in the shell due to the lug axial force are negligible, no more results and comparisons concerning this case will be presented.

With the elastic evaluation of the stresses in the local region, the radial forces in the lugs, corresponding to different stress assessment lines, can be estimated. The estimated radial forces are shown in Table F. For instance, for the stress assessment line L1, at a distance of $0.1\sqrt{Rt}$, the radial force of 1.77 MN on the lug (disregarding the internal pressure in the cylinder) causes a stress intensity of 377 MPa. Classifying such stress as P_L (local primary membrane stress) and, limiting it to the allowable stress limit of $1.5 S_m = 276$ MPa, the estimated allowable radial force turns out to be 1.30 MN = $(276/377) \times 1.77$. From the elastic FEA and considering the same loading conditions described in Table D, the membrane plus bending stress intensities reported in Table G can be figured out.

Considering the membrane plus bending stress intensities classified in the local

Considering the membrane plus bending stress intensities classified in the local region as $P_L \pm P_B$ (local primary membrane plus bending stress) with the corresponding ASME allowable limit of $1.5 S_m = 276$ MPa, one can evaluate the allowable radial forces from elastic FEA using the same procedure described above. The results are summarized in Table H.

TABLE-F: Allowable radial forces, from elastic FEA (membrane stress as P_L)

		L1 - $0.1\sqrt{Rt}$	L2 - $0.5\sqrt{Rt}$	L3 - $1.0\sqrt{Rt}$
radial forces in the lugs	with pressure (10 MPa)	1.47	3.57	4.51
	without pressure	1.30	2.42	3.94

TABLE G: Membrane plus bending stress intensities (MPa), from elastic FEA

		L1 - $0.1\sqrt{Rt}$	L2 - $0.5\sqrt{Rt}$	L3 - $1.0\sqrt{Rt}$	L4 - $2.0\sqrt{Rt}$
radial forces in the lugs	with pressure (10 MPa)	1444	952	803	682
	without pressure	1541	971	705	568

TABLE-H: Allowable radial forces from elastic FEA (membrane+bending as $P_L \pm P_B$)

		L1 - $0.1\sqrt{Rt}$	L2 - $0.5\sqrt{Rt}$	L3 - $1.0\sqrt{Rt}$
radial forces in the lugs	with pressure (10 MPa)	0.36	0.54	0.63
	without pressure	0.32	0.50	0.69

TABLE I: Allowable radial forces from elastic FEA (membrane plus bending as $P+Q$)

		1 - $0.1\sqrt{Rt}$	2 - $0.5\sqrt{Rt}$	3 - $1.0\sqrt{Rt}$
radial forces in the lugs	with pressure (10 MPa)	0.72	1.08	1.26
	without pressure	0.63	1.01	1.39

If one considers the membrane plus bending stress intensities classified as $P + Q$ (primary plus secondary stress) with the limit $3.0 S_m = 552$ MPa the resultant allowable radial force on the lug are calculated and the results shown in Table I.

CONCLUDING REMARKS

This paper has presented the finite element results of elastic and elastic-plastic analyses of axisymmetric and tridimensional geometries. The analyses were directed towards the calculation of allowable loads in support skirts with different attachment angles and also in a complex lug-cylinder configuration. Depending on the stress assessment and stress classification adopted for the elastic results interpretations, different allowable loads were obtained.

For the axisymmetric skirt support, considering Table-B, it can be observed that the simple approach, the elastic FEA, and the lower bound FE limit load analyses gave extremely different results. It is obvious from the calculations that the stress classifications and the stress assessment methods influence the determination of the allowable loads. Taking the Code definition of Limit-Load Analysis as the basis for design, and comparing the different allowable loads, it can be stated that: **(i)** The "simple" approach gave greater allowable loads; **(ii)** categorizing the membrane near structural discontinuity as PL also resulted in greater allowable loads; **(iii)** taking membrane + bending near structural discontinuity as primary, produced smaller allowable loads; **(iv)** considering membrane + bending at structural discontinuity as primary + secondary (P + Q) resulted in greater allowable loads. Notice that PM, PL, and PB limits are related to plastic collapse, while P + Q is related to fatigue and incremental plastic deformation. These conclusions are based on the SCL's of Figure 1. Those SCL's were selected on the basis of the designer's expertise.

Examining Table-B, further observations can be taken: **(i)** For the skirt with $\alpha=18^\circ$, the results confirm the observations and the conclusions given in [1]. However, we observe that in this case, both the "simple" theory and the elastic FEA results (away from the cone-cylinder juncture) approximate the plastic collapse end-load which is controlled by the higher stresses at the juncture. **(ii)** For the skirt with $\alpha = 45^\circ$, the stress assessment based on elastic FEA (M as PL) shows an allowable load slightly greater than the FE limit-load analysis (14637psi against 12467psi). In this case, the allowable load based on the "simple" theory is much greater than the FE limit-load analysis (26700psi against 12467psi). The elastic FEA (SCL-E) approximates the plastic collapse in the skirt much better than the simple beam theory. **(iii)** For the skirt with $\alpha = 25^\circ$, neither the "simple" theory nor the elastic FEA gave allowable loads closed to the FE limit-load analysis (26700psi and 25238psi against 20466psi). This case, among other cases, should be looked at with care because it may lead the stress analyst to non conservative designs or high costs.

For the cases studied involving complex 3D geometries as the lug-cylinder attachment analyzed in this paper, some observations can be drawn from the analyses performed. **(i)** Axial forces on the lugs have little influence in the stress distribution in the shell. **(ii)** The allowable axial forces in the lugs considering a simplified elastic analysis - and the recommendations prescribed in the limits of "NB-3227.2 Pure Shear" of the ASME code - gives good agreement with the allowable axial force obtained from the elastic-plastic FEA - with the limits of "NB-3228 Applications of Plastic Analysis" of the ASME code. In fact, 1.05 MN for the elastic analysis against 1.11 MN for the elastic-plastic FEA. **(iii)** For the radial

force on the lug, performing the same type of comparison as done in item "ii" did not yield good agreement - 4.42 MN (elastic) versus 1.77 MN (plastic). (iv) From elastic FEA, the allowable radial forces in the lugs - obtained from the stress assessment lines near $0.1\sqrt{Rt}$ away from the edge of the lug-cylinder attachment, and considering the membrane stresses as P_L with the limit of $1.5 S_m$ - are about 70-80 % of the allowable force obtained from elastic-plastic FEA. This is the assessment lines where the radial allowable force is better approximated when considering elastic and elastic-plastic FEA. (v) The comparison in terms of membrane plus bending stresses indicates that the results of elastic FEA are much smaller than those from elastic-plastic FEA.

The results obtained in this paper suggest that for almost all cases here studied the use of elastic analysis and the limits of the ASME code are conservative when compared with elastic-plastic analysis checks. The different results, however, revealed the lack of appropriate guidelines in the ASME recommendations for appropriate stress assessment and verification of complex 3D geometries. In the present stage of automation, where the engineering offices use massive FE computation, including 3D modeling for design and analysis of pressure vessel components, it is wise that ASME should develop, at least in a general sense, recommendations to guide the stress analyst to safety decisions.

REFERENCES

- [1] Hollinger, G. L. and Hechmer, J. L., 1993, "Three Dimensional Stress Evaluation Guidelines Progress Report," PVP-Vol. 277.
- [2] Hollinger, G. L. and Hechmer, J. L., 1986, "Three Dimensional Stress Criteria - A Weak Link in Vessel Design and Analysis". PVP-Vol. 109.
- [3] ASME, 1968, "Criteria of the ASME Boiler and Pressure Vessel Code for Design by Analysis in Section III and VIII, Division 2, The American Society of Mechanical Engineering New York, NY.
- [4] ASME, 1989, "Section III Rules for Construction of Nuclear Power Plant Components, Division 1 - Subsection NB, Class 1 Components." The American Society of Mechanical Eng., New York, NY.
- [5] ASME, 1989, "Section III Rules for Construction of Nuclear Power Plant Components, Division 1- Appendices". The American Society of Mechanical Engineers, New York, NY.
- [6] Hollinger, G. L. and Hechmer, J. L., 1991, "Three Dimensional Stress Criteria" PVP-Vol. 210-2
- [7] ASME 1992. ASME Boiler and Pressure Vessel Code, Section III, Nuclear Power Plant Components. New York: ASME.
- [8] ASME 1969. Criteria of the ASME Boiler and Pressure Vessel Code for Design by Analysis in Section III and Section VIII, Division 2. New York: ASME.
- [9] Hollinger, G. L. & J. L. Hechmer 1994. *Three Dimensional Stress Evaluation Guidelines Progress Report. Recertification and Stress Classification Issues*: 95-102. New York: ASME.
- [10] SASI 1992. *ANSYS User's Manual for revision 5.0*. Houston, PA, USA: SASI.